NASA Technical Memorandum 86930

NASA-TM-86930 19850009816

A Study of Spectrum Fatigue Crack Propagation in Two Aluminum Alloys II—Influence of Microstructures

Jack Telesman
Lewis Research Center
Cleveland, Ohio

and

Stephen D. Antolovich
Georgia Institute of Technology
Atlanta, Georgia

January 1985

NASA

A STUDY OF SPECTRUM FATIGUE CRACK PROPAGATION IN TWO ALUMINUM ALLOYS
II - INFLUENCE OF MICROSTRUCTURES

Jack Telesman
National Aeronautics and Space Administration
Lewis Research Center
Cleveland, Ohio 44135

and

Stephen D. Antolovich
Georgia Institute of Technology
Fracture and Fatigue Research Laboratory
Atlanta, Georgia 30332

SUMMARY

An investigation to determine the important metallurgical factors that influence both constant amplitude and spectrum crack growth behavior in aluminum alloys was performed. The effect of microstructural features such as grain size, inclusions, and dispersoids was evaluated. It was shown that at lower stress intensities, the I/M 7050 alloy showed better FCP resistance than P/M 7091 alloy for both constant amplitude and spectrum testing. It was suggested that the most important microstructural variable accounting for superior FCP resistance of 7050 alloy is its large grain size. It was further postulated that the inhomogenous planar slip and large grain size of 7050 limit dislocation interactions and thus increase slip reversibility which improves FCP performance. The hypothesis was supported by establishing that the cyclic strain hardening exponent for the 7091 alloy is higher than that of 7050.

INTRODUCTION

The continuous evolution of the military and civilian aircraft structures has led to significant improvements in aircraft performance. However, improvements in design characteristics of the newly developed aircraft structures are ultimately limited by the properties of presently used materials. Thus, there is a well-defined need to understand and improve the properties of currently used aircraft materials.

In recent years, the main focus in aluminum alloy development for aircraft structures has centered on both powder metallurgy (P/M) alloys as well as optimization of composition of ingot metallurgy (I/M) alloys. Two of the best known new alloys developed by these processes are P/M 7091 and I/M 7050. Due to differences in processing, they have very different microstructures (e.g., grain size, inclusion, dispersoid, and oxide composition and distribution) thus lending themselves to an investigation of the effect of these metallurgical variables on fatigue crack propagation (FCP).

Fatigue crack propagation behavior under variable amplitude (spectrum) loading is widely used in selecting materials for aircraft structures. The use of spectrum FCP data is more realistic than use of constant amplitude information since load sequences can have a considerable effect on FCP rates.

However, at present, the interactions between alloy microstructure and variable amplitude fatigue are not well-understood.

The purpose of this investigation was to identify metallurgical factors in aluminum alloys, which control FCP behavior under both constant amplitude and spectrum loading.

EXPERIMENTAL PROCEDURES

Most of the experimental procedure dealing with constant amplitude and spectrum testing, metallography, and fractography were described in the preceding companion paper. The experimental procedure dealing exclusively with this paper only is described below.

Low Cycle Fatigue (LCF)

Testing was performed using a closed loop, servocontrolled hydraulic MTS machine. All tests were strain controlled, with the strain being monitored using an axial extensometer. Two different plastic strain ranges were used ($\Delta\varepsilon_p$ = 0.15 percent and $\Delta\varepsilon_p$ = 2.0 percent). All tests were fully reversed using a ramp wave form and performed at a frequency of 0.25 Hz in an ambient environment. The testing was performed in order to analyze the deformation structure of two different strain ranges and thus no strain-life data was obtained.

Cyclic strain hardening exponent, n', was calculated by fitting the following equation to a single stable LCF stress-strain loop:

$$\frac{\sigma}{2} = K(\varepsilon_p/2)^{n'} \qquad (1)$$

where σ and ε_p are respectively cyclic stress and plastic strain ranges, K is a constant. The values of σ and ε_p were obtained by putting the origin at the lower end of the hysteresis loop.

Transmission Electron Microscopy (TEM)

Wafers 0.25 mm (0.01 in) thick were cut from the specimens. A slow feed rate and ample coolant were used to prevent specimen heating and possible changes of the substructure.

The wafers were ground on 300 grit silicon carbide paper to thickness of 0.13 mm (0.005 in). The foils were then electro-polished by a dual-jet unit until suitable for viewing. In the case of spectrum FCP specimens, the fracture surface was blocked off by tape, so that the electro-polishing occurred only from one side. In this way the foil was extremely close to the fracture surface and the fatigue deformation substructure could be imaged.

The electrolyte was:

25 ml HNO_3 (concentrated)

75 ml methanol

This solution was cooled to -30 °C. The polishing conditions were approximately 20 V and 100 to 150 mA.

The foils were examined using an accelerating voltage of 150 KV on a JEOL JEM-200 A microscope.

RESULTS AND DISCUSSION

Initial Microstructure

The grain structure of the 7050 alloy is shown in figure 1 and reveals large pancake shaped grains (up to 200 μm long in the rolling direction) as well as small subgrains (as confirmed by TEM analysis). The volume fraction of the recrystallized structure is approximately 55 percent as determined by the quantitative stereological methods (ref. 1). This is comparable to the results obtained by Sanders and Starke (ref. 2) who estimated that 40 percent of the structure in a similar 7050 alloy was recrystallized. The microstructure of 7050-T7 alloy showing features such as subgrains, precipitate free zones (PFZ), dispersoid and precipitate size, and distribution is shown in figure 2. The subgrain size ranges from 1 to 5 μm. The spherical dispersoids of alloy 7050 have been identified as Al_3Zr.

In contrast to the 7050 alloy, the grain structure of 7091 is very small, (fig. 3), with pancake shaped grains measuring from 5 to 20 μm. The P/M alloy revealed no observable large constituent particles. This is due to the high quenching rate of P/M alloys (10^5 to 10^6 K/sec) which minimizes segregation and consequently the formation and growth of constituent particles (ref. 3). The subgrain size of 7091, (fig. 4), ranges from 1 to 5 μm and is thus comparable to that of 7050. Also alloy 7091 has a substantially greater density of dispersoid particles than I/M 7050. The dispersoids in 7091 have been identified as Co_2Al_9 (ref. 3) and are spherical to oval in shape with the approximate diameter of 0.1 to 0.5 μm.

Fatigue Crack Propagation Results

Comparison of constant amplitude FCP results, (fig. 5), reveals that the 7050 alloy is significantly more FCP resistant at the lower stress intensities than 7091. However, the gap narrows as the stress intensity becomes larger. It should be pointed out that the lower stress intensity region behavior is more important since a significantly larger portion of the fatigue life occurs there. The results obtained in this study are in agreement with those obtained by others (refs. 3 to 6) who also showed that the FCP resistance of aluminum P/M alloys under constant amplitude loading is inferior to the comparable composition I/M alloys.

The results of spectrum FCP testing are shown in figures 6 and 7. For both spectra, the spectrum FCP rates of alloy 7050 are significantly lower than those of 7091 at the more important lower maximum stress intensities, (K_{max}), where most of the fatigue life is spent. As K_{max} increases, the gap in the spectrum FCP rates diminishes, to a point where, at higher K_{max}, a crossover occurs and the 7091 alloy exhibits slightly better FCP resistance. These trends were the same for both load histories and the crossovers occurred at comparable K_{max} levels (30 to 40 MPa$\sqrt{m}$). Thus, for all three different load

histories studied in this program (i.e., constant amplitude, TD spectrum, and TC spectrum), small grain P/M 7091-T7E70 alloy showed inferior FCP resistance at the lower stress intensities in comparison to the large grain I/M 7050-T73651 alloy.

Possible explanations as to the reasons why the microstructure of 7050 alloy results in superior FCP resistance in comparison to the microstructure of 7091 alloy can be obtained by considering the fractographic and TEM analysis.

TEM Results

An analysis of the deformed structures was performed on both alloys. Foils were prepared from both the FCP and LCF specimens. The deformation mode for a given alloy was the same for both low and high strain LCF specimens as well as for the FCP specimens.

For the 7050-T7 alloy, deformation was found to occur by both nonhomogenous slip which resulted in formation of slip bands, (fig. 8), and homogenous slip, (fig. 9). In the case of 7091-T7 alloy only homogenous type deformation was observed, (fig. 10). These results are in agreement with a generally recognized trends where the reduced grain size usually leads to a more homogenous deformation (refs. 5 and 6).

Another factor which might have lead to inhomogenous deformation in the 7050 alloy was the presence of some degree of coherency of the precipitates with respect to the matrix. Overaging, which was performed by the T7 treatment, is known to reduce the coherency of the precipitates and lead to enhancement of homogenous deformation (ref. 7). However, some coherency was still present in the 7050 alloy, since regions of inhomogenous deformation were detected. The existance of some degree of coherency of the precipitates in the 7050 alloy can explain the somewhat higher than expected tensile properties of this alloy (i.e., table II, part I).

Fractography

A fractographic analysis revealed large differences in the failure mode between the 7091 and 7050 alloys. For instance, (as shown in fig. 11), 7050 alloy subjected to spectrum loading, exhibited crystallographic features and cleavage-like facets, as well as irregularly spaced striations. In comparison, the 7091 P/M alloy subjected to similar loading history and stress intensities failed along small noncrystallographic plateaus, (fig. 12).

One of the most important aspects of the fractographic analysis of the two alloys subjected to both constant amplitude and spectrum loading is the very different striation character of the two alloys. A direct comparison of the striation character of the two alloys subjected to the same load history, environment and stress intensity is shown in figure 13. Striations in the I/M 7050 alloy are clearly visible, well-developed and "ductile" in character, whereas striations in the P/M 7091 are "brittle" and considerably less developed. Striation profile as well as any other fracture surface features, are characteristic of the amount of deformation the material can absorb prior to fracture. Thus, well-developed "ductile" striations are characteristic of material capable of absorbing larger amounts of deformation (microductility) than the "brittle" striation forming material.

It has been shown by Lynch (ref. 8), Thompson and Craig (ref. 9), and Forsyth (ref. 10) that the character of striations can be tied in to FCP rates. The more brittle the striation character, (usually caused by aggressive environments) the higher the FCP rates.

Since crack propagation to a large extent occurs by striation forming mechanisms, the character of striations might be correlated to the fatigue damage mechanism and the corresponding crack propagation rates. Thus the reasons behind the greater microductility in 7050 alloy should shed important clues in understanding FCP process.

Relationship Between Deformation Mode and Microstructure

A possible explanation for the difference in striation character (i.e., microductility) of the two alloys is a mechanism suggested by Lindingkeit et al. (ref. 11). They suggested that decrease in grain size created more obstacles (i.e., grain boundaries) for dislocation movement thus decreasing the slip reversibility. The lack of slip reversibility increases dislocation interactions and increases FCP rates. This mechanism should result in higher dislocation density and higher cyclic strain hardening at the crack tip for the 7091 alloy. Several investigators (refs. 12 to 14) had shown that increasing the dislocation density increases FCP rates. An attempt was made in this program to compare the dislocation densities near the crack tip for the two alloys. However, due to the difficulties encountered in obtaining a sharp image of a large number of entangled dislocations in the strained aluminum specimens, it was impossible to quantify the dislocation densities.

The difference in the slip mode of the two alloys as was observed by the TEM examination also support the suggestion that slip reversibility is enhanced in the 7050 alloy. Inhomogenous slip was present in 7050 while 7091 alloy exhibited only homogenous slip.

In order for inhomogenous planar deformation to occur in the 7050 alloy, some degree of coherency of the precipitates had to exist. The presence of the semicoherent precipitates will have a tendency to localize the slip since deformation on an active slip plane, with each successive cycle, will require less shear stress for the dislocations to pass through the precipitates. This process should limit cyclic hardening. In addition, the dislocation interactions on the widely separated slip planes should be limited. This should result in significantly fewer dislocation interactions, and a greater slip reversibility. Due to the higher slip reversibility considerably fewer new dislocations will be formed during cycling and the rate of damage accumulation by this mechanism should be reduced, thus increasing the microductility of the 7050 alloy.

Only homogenous slip was observed in 7091 alloy, indicating lack of coherency of the precipitates. Thus slip occurs on many closely spaced planes. The small distance between slip planes increases dislocation interactions and limits slip reversibility.

If this description of the behavior of the two alloys is accurate, then small grain size, increased dislocation interactions, and reduced slip reversibility in 7091 alloy should result in greater cyclic hardening.

The cyclic stress-strain curves of the two alloys were obtained from the LCF test results, (fig. 14). The cyclic strain hardening exponents (n') are respectively 0.26 and 0.17 for the 7091 and 7050 alloy. Thus, 7091 does exhibit higher strain hardening than 7050 supporting the hypothesized behavior.

The trend of the FCP results is also in agreement with the model suggested by Saxena and Antolovich (ref. 15).

In this model the FCP rate is given by:

$$\frac{da}{dN} = \frac{C}{(\sigma'_{ys}\epsilon'_f E)^{1/\beta}} \cdot \frac{1}{\ell^{1/\beta-1}} \Delta K^{2/\beta} \qquad (2)$$

where

σ'_{ys} = cyclic yield strength

ϵ_f' = true fracture strain

E = Young's Modulus

ℓ = process zone size

β = Coffin-Manson exponent

C = material constant

In a qualitative sense, the larger the process zone, the lower the crack growth rate, other factors being equal. The process zone is larger for materials exhibiting inhomogenous slip and larger grain size. On this basis the FCP rate would be expected to be lower for 7050 and this is indeed the case as seen in figures 5 to 7.

Effect of Secondary Particle

The I/M 7050 alloy contained a significant number of large secondary particles (up to 30 μm long), while the P/M 7091 alloy contained very few of these type of particles.

The influence of these particles (inclusions) on FCP at different stress intensity ranges was investigated by comparing the volume fraction of broken secondary particles on the fracture surface and a randomly chosen plane of the same orientation away from the fracture surface. This analysis indicated that for both constant amplitude and spectrum specimens, at lower stress intensities, the volume fraction of the broken inclusions on the fracture surface was approximately 0.11 which was comparable to that on the randomly chosen plane (volume fraction approximately 0.10). Only at higher stress intensities was the volume fraction of broken particles significantly higher than that of a randomly chosen plane. This analysis indicates that at lower stress intensities, the crack tip does not preferentially follow inclusions and thus it could be inferred that these particles only have a secondary effect on FCP rates at the lower stress intensities.

Alloy 7050 contains Al_3Zr types of dispersoid particles, while the 7091 alloy contains Co_2Al_9 particles of the same nature (refs. 4 and 16). No

direct comparison of the effect of the amount of these particles on FCP rates was attempted in this work. However, the work by R.E. Sanders and Otto (ref. 3) does shed some light on the effect of Co_2Al_9 dispersoids on FCP rates in 7091 alloy. They varied the cobalt content from zero to 0.8 percent thus changing the distribution density of these dispersoids without changing the grain size. No difference in FCP between any of these alloys was found thus indicating that the dispersoids have no significant effect on the FCP rates.

Since the role of the Al_3Zr dispersoids in the 7050 alloy is comparable to the Co_2Al_9 dispersoids, it is reasonable to assume that they also have a negligible effect on FCP rates. It should be pointed out that even though the dispersoid particles themselves might not have a significant effect on FCP rates, their ability to control grain size in turn can be very important in determining FCP behavior.

SUMMARY and CONCLUSIONS

An investigation to determine the important metallurgical factors that influence both constant amplitude and spectrum FCP behavior in two 7XXX series aluminum alloys was performed.

Several observations can be made regarding the FCP behavior of the two alloys:

1. For all three load histories (constant amplitude, TC and TD spectra) I/M 7050-T7 alloy exhibited better FCP resistance than the P/M 7091-T7 alloy at lower and intermediate stress intensities. At higher stress intensities the differences diminished.

2. The most important difference in fractographic appearance between the two alloys was the striation profile. I/M 7050 alloy exhibited "ductile" striations indicating the ability of this alloy to absorb a large amount of plastic deformation. P/M 7091 exhibited "brittle" striations indicating a significantly lesser ability to absorb deformation.

3. Alloy 7050-T7 exhibited both homogenous and nonhomogenous plastic deformation, while 7091-T7 exhibited only homogenous deformation.

4. It was postulated that the nonhomogenous planar slip and large grain size of 7050 limit dislocation interactions, and thus increase the slip reversibility which improves FCP performance in both constant amplitude and spectrum cycling.

5. Small grain size and homogeneous slip in 7091 lead to more dislocation interactions and limited slip reversibility. These factors tend to reduce the fatigue crack propagation resistance of 7091 relative to 7050.

6. The above two conclusions were supported by a higher cyclic strain hardening exponent for the 7091 alloy and more rapid crack growth in agreement with theoretical models.

REFERENCES

1. Underwood, E.E.; and Starke, E.A., Jr.: Quantitative Stereological Methods for Analyzing Important Microstructural Features in Fatigue of Metals and Alloys. Fatigue Mechanisms (ASTM STP-675), 1979, pp. 633-682

2. Sanders, R.E., Jr.; and Starke, E.A., Jr.: The Effect of Intermediate Thermomechanical Treatments on the Fatigue Properties of a 7050 Aluminum Alloy. Metall. Trans. A, vol. 9, no. 8, Aug. 1978, pp. 1087-1100.

3. Sanders, R.E., Jr.; and Otto, W.L., Jr.: The Fatigue Resistance of High Strength 7xxx P/M Aluminum Alloy Extrusions. 1978-1979 National Powder Metallurgy Conference Proceedings, James Hoffman, ed., Progress in Powder Metallurgy, vol. 35, Metal Powder Industries Federation, 1979, pp. 295-311.

4. Lyle, J.P.; and Cebulak, W.S.: Powder Metallurgy Approach for Control of Microstructure and Properties in High Strength Aluminum Alloys. Metall. Trans. A., vol. 6, no. 4, Apr. 1975, pp. 685-706

5. Lawley, A.; and Koczak, M.J.: A Fundamental Study of Fatigue in Powder Metallurgy Aluminum Alloys. Final Technical Report Mar. 1977-Feb. 1981, Drexel Unic., Aug. 1981. (AFOSR 77-3247, AD-A105080.)

6. Voss, David P.: Structure and Mechanical Properties of Powder Metallurgy 2024 and 7075 Aluminum Alloys. EOARD TR-80-1, Oct. 1979. (AD-A087/6/1.)

7. Starke, E.A., Jr.; and Luetjering, G.: Cyclic Plastic Deformation and Microstructure. Fatigue and Microstructure, ASM, 1978, pp. 205-243.

8. Lynch, S.P.: Mechanisms of Fatigue and Environmentally Assisted Fatigue. Fatigue Mechanisms (ASTM STP-675), Jeffrey Tse-Wei Fong, ed., ASTM, 1979, pp. 174-213.

9. Thompson, K.R.L.; and Craig, J.V.: Fatigue Crack Growth Along Cleavage Planes in an Aluminum Alloy. Metall. Trans., vol. 1, no. 4, Apr. 1970, pp. 1047-1049.

10. Forsyth, P.J.E.: Fatigue Damage and Crack Growth in Aluminum Alloys. Acta Metall., vol. II, no. 7, July 1963, pp. 703-716.

11. Lindingkeit, J., et al.: The Effect of Grain Size on the Fatigue Crack Propagation Behavior of Age-Hardened Alloys in Inert and Corrosive Environment. Acta. Metall., vol. 27, no. 11, Nov. 1979, pp. 1717-1726.

12. Broek, D.; and Bowles, C.Q.: The Effect of Precipitate Size on Crack Propagation and Fracture of an Al-Cr-Mg Alloy. J. Inst. Met., vol. 99, 1971, pp. 255-257.

13. Staley, J.T.: Influence of Microstructure on Fatigue and Fracture of Aluminum Alloys. Aluminum, vol. 55, no. 4, Apr. 1979, pp. 277-281.

14. Kang, T.S.; and Liu, M.W.: Eng. Fract. Mech., vol. 6, no. 4, Dec. 1974, pp. 631-638.

15. Saxena, Ashok; and Antolovich, Stephen D.: Low Cycle Fatigue, Fatigue Crack Propagation and Substructures in a Series of Polycrystalline CU-Al Alloys. Metall. Trans. A, vol. 6, no. 9. Sept. 1975, pp. 1809-1828.

16. Otto, W.L., Jr.: Metallurgical Factors Controlling Structure in High Strength P/M Products. Final Tech. Rep. Apr. 1974-Oct. 1975, Aluminum Co. of America, May 1976. (AFML-TR-76-60, Ad-A030606.).

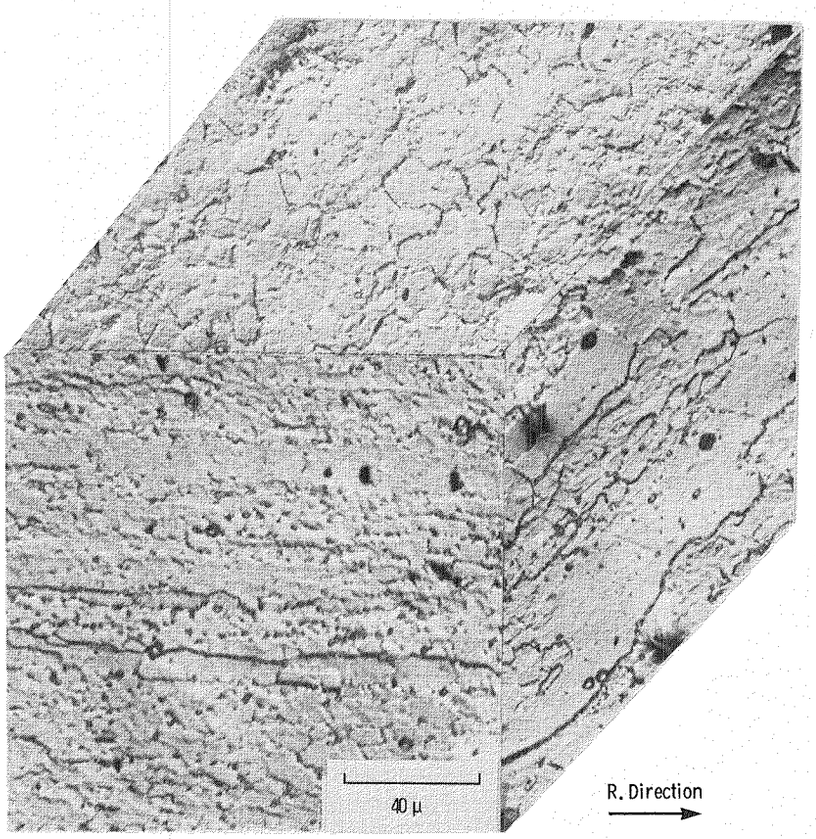

Figure 1. - Grain structure of 7050 alloy.

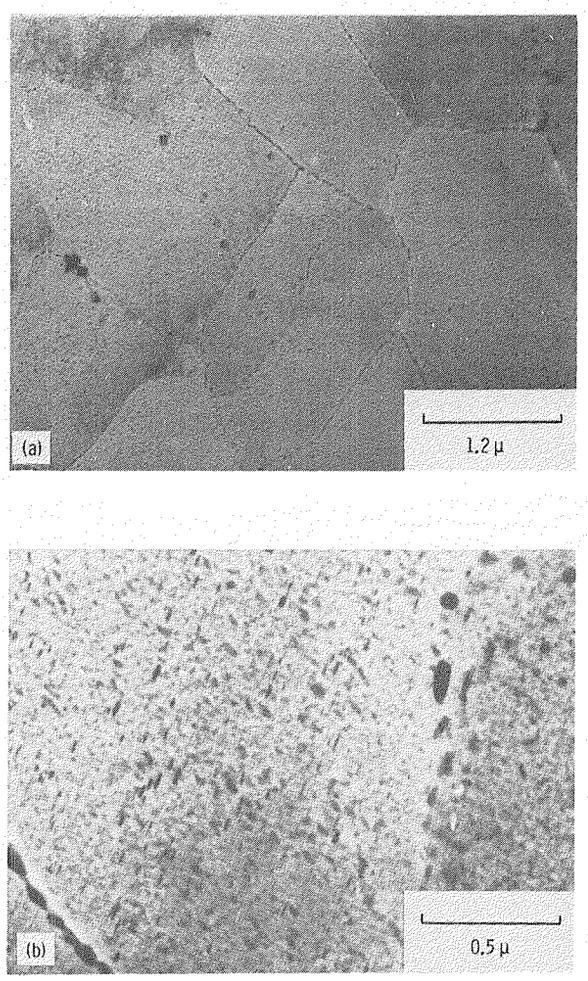

Figure 2. - TEM micrographs of 7050 alloy showing subgrains, dispersoids, and precipitates.

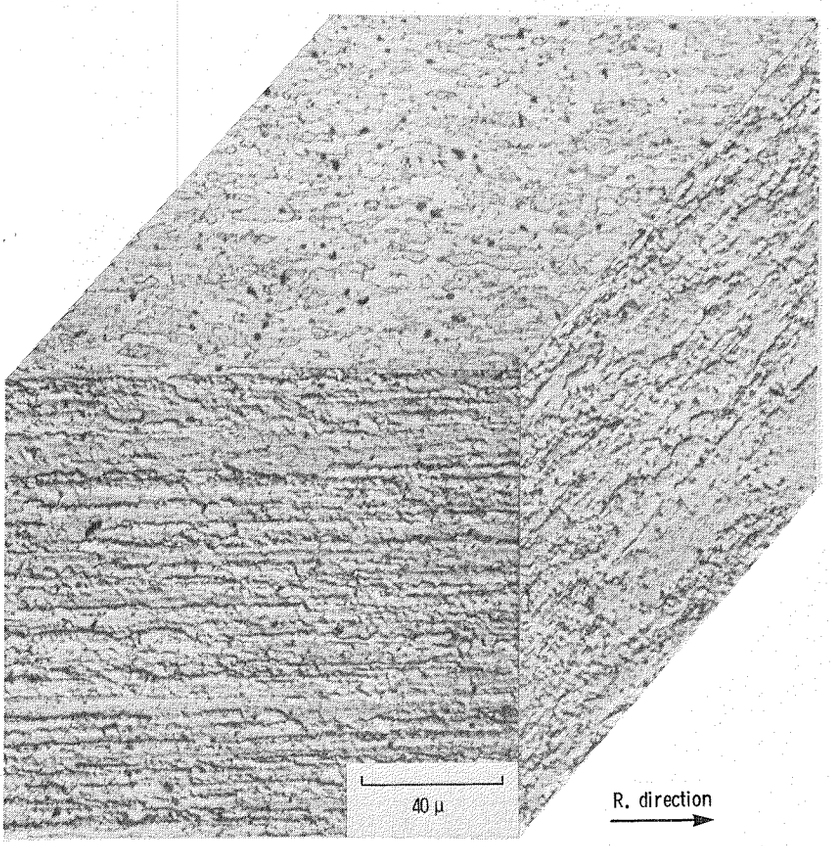

Figure 3. - Grain structure of 7091 alloy.

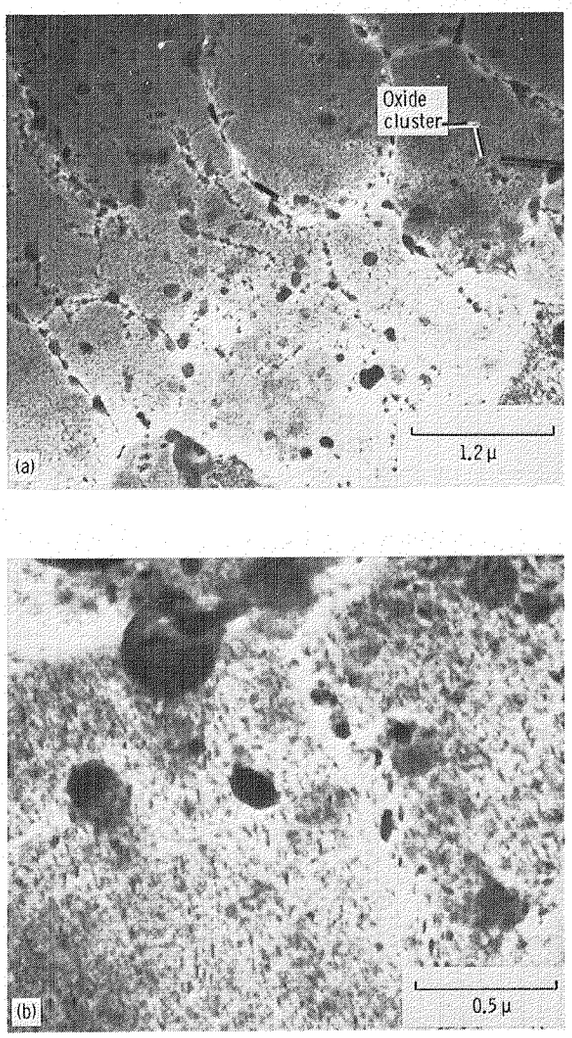

Figure 4. - TEM micrographs of 7091 alloy showing subgrains, dispersoids, and precipitates.

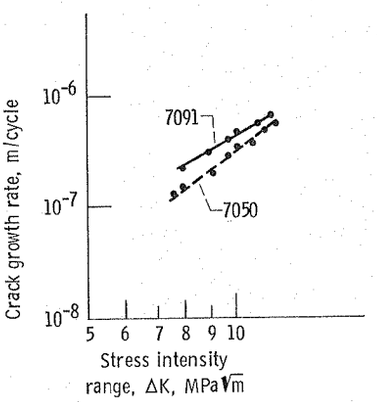

Figure 5. - Comparison of constant amplitude FCP results for the two alloys.

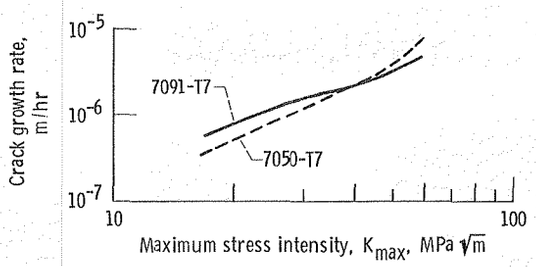

Figure 6. - FCP results for the two alloys subjected to a TD spectrum.

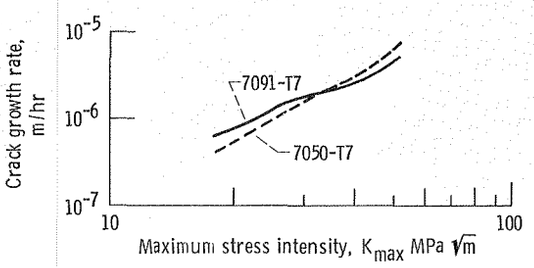

Figure 7. - FCP results for the two alloys subjected to a TC spectrum.

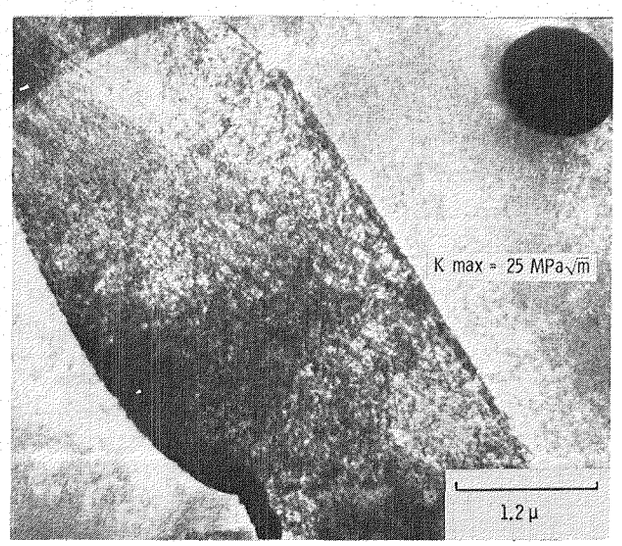

Figure 8. - Inhomogenous deformation in 7050 alloy. Foil obtained directly below the fracture surface of a spectrum specimen.

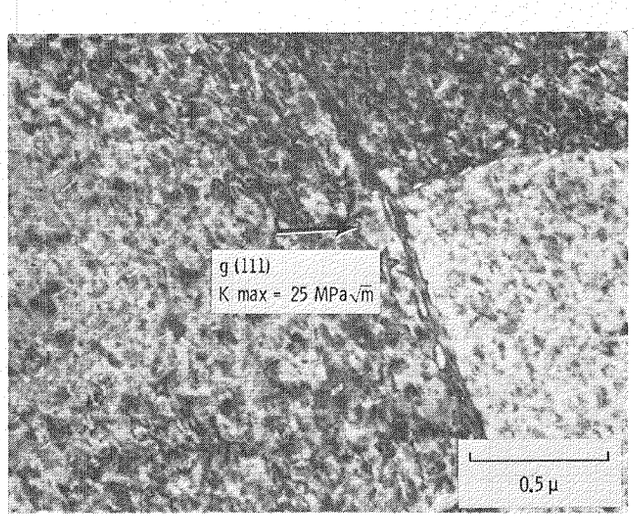

Figure 9. - Homogenous deformation in 7050 alloy. Foil obtained directly below the fracture surface of a spectrum specimen.

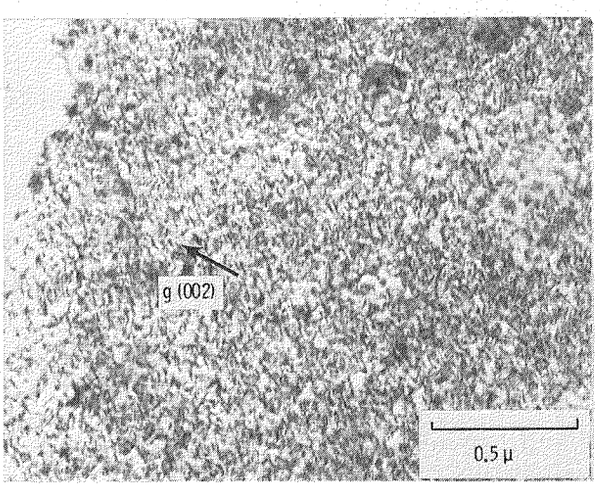

Figure 10. - Homogenous deformation in 7091 alloy. All foils from this material had similar deformation substructures.

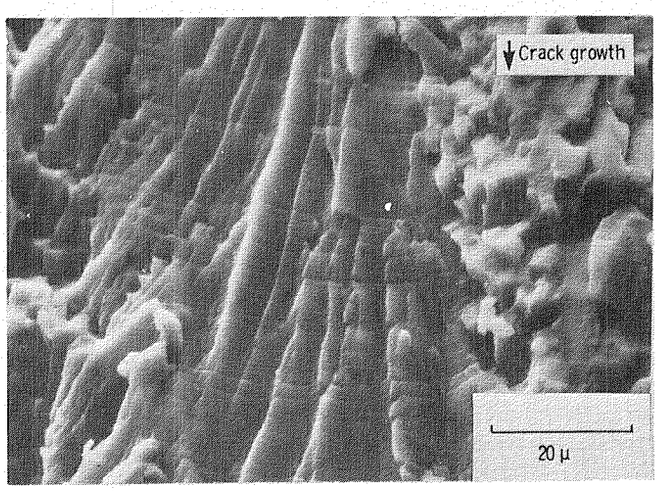

Figure 11. - 7050 alloy subjected to a TD spectrum. Typical fracture surface of this alloy showing irregularly spaced striations and cleavage-like facets.

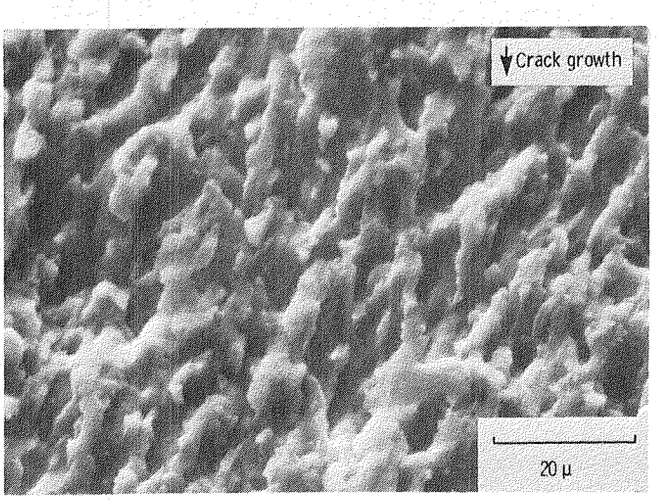

Figure 12. - 7091 alloy subjected to a TD spectrum. Typical fracture surface of this alloy showing small noncrystallographic plateaus.

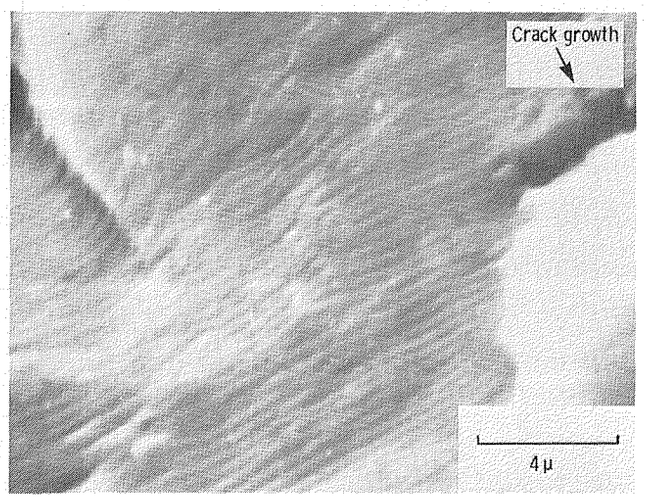

(a) 7050.

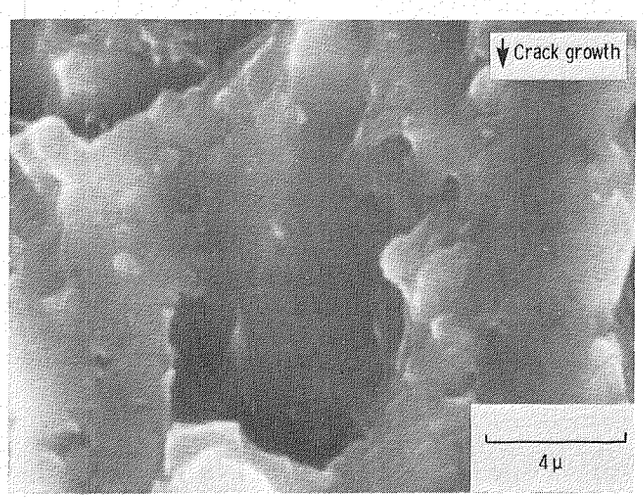

(b) 7091.

Figure 13. - Comparison of striation profiles of the two alloys subjected to identical load histories, (ΔK = 13 MPa$\sqrt{m}$).

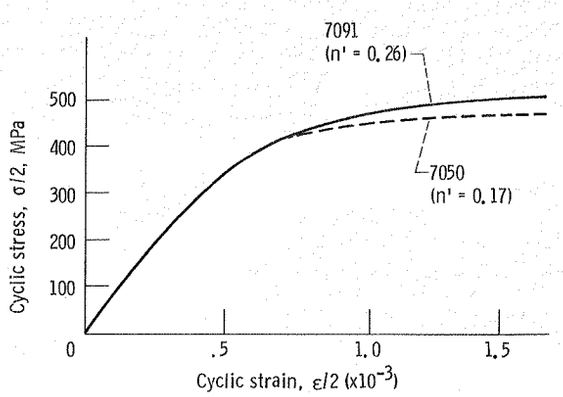

Figure 14. - Comparison of cyclic strain hardening exponents of the two alloys. Cyclic data obtained by evaluating a single stable hysteresis loop of each alloy.

1 Report No	2 Government Accession No	3 Recipient's Catalog No
NASA TM-86930		

4 Title and Subtitle	5 Report Date
A Study of Spectrum Fatigue Crack Propagation in Two Aluminum Alloys II - Influence of Microstructures	January 1985
	6 Performing Organization Code 505-33-7C
7 Author(s) Jack Telesman and Stephen D. Antolovich	8 Performing Organization Report No E-2439
	10 Work Unit No
9 Performing Organization Name and Address National Aeronautics and Space Administration Lewis Research Center Cleveland, Ohio 44135	11 Contract or Grant No
	13 Type of Report and Period Covered Technical Memorandum
12 Sponsoring Agency Name and Address National Aeronautics and Space Administration Washington, D.C. 20546	14 Sponsoring Agency Code

15 Supplementary Notes

Jack Telesman, NASA Lewis Research Center; Stephen D. Antolovich, Georgia Institute of Technology, Fracture and Fatigue Research Laboratory, Atlanta, Georgia 30332.

16 Abstract

An investigation to determine the important metallurgical factors that influence both constant amplitude and spectrum crack growth behavior in aluminum alloys was performed. The effect of microstructural features such as grain size, inclusions, and dispersoids was evaluated. It was shown that at lower stress intensities, the I/M 7050 alloy showed better FCP resistance than P/M 7091 alloy for both constant amplitude and spectrum testing. It was suggested that the most important microstructural variable accounting for superior FCP resistance of 7050 alloy is its large grain size. It was further postulated that the inhomogenous planar slip and large grain size of 7050 limit dislocation interactions and thus increase slip reversibility which improves FCP performance. The hypothesis was supported by establishing that the cyclic strain hardening exponent for the 7091 alloy is higher than that of 7050.

17 Key Words (Suggested by Author(s))	18 Distribution Statement
Microstructure; Fatigue crack propagation; Spectrum loading; Aluminum; Powder metallurgy	Unclassified - unlimited STAR Category 26

19 Security Classif (of this report)	20 Security Classif (of this page)	21 No of pages	22 Price*
Unclassified	Unclassified		

*For sale by the National Technical Information Service, Springfield, Virginia 22161

End of Document